Supplementary Information for

Optically induced charge separation at the naphtalenediimide-phenothiazine interface

Physical Chemistry Chemical Physics

Thomas Trepl,[a] Renan Gabriel de Assis,[b] Christine M. Isborn,[c]
Thiago Branquinho de Queiroz,*[b] and Stephan Kümmel*[a]

* Corresponding authors
[a]Theoretical Physics IV, University of Bayreuth, Bayreuth 95440, Germany
E-mail: stephan.kuemmel@uni-bayreuth.de
[b]Center for Natural and Human Sciences, Federal University of ABC, 09210-580 Santo André-SP, Brazil
E-mail: thiago.branquinho@ufabc.edu.br
[c]Department of Chemistry and Biochemistry, University of California Merced, Merced, California 95343, USA

Contents

S1 Detailed simulation information

In this section we give detailed information about the simulation parameters and list the electronic structure programs.

TBP, NDI-silane

Geometry Optimization

Software: Q-Chem[1], Functional: M06-2X[2], Basis set: 6-31G**
Optimization thresholds: Gradient-Max $< 3 \cdot 10^{-4}$ a.u. & $\Delta E < 1 \cdot 10^{-6}$ a.u.

Optimal tuning

Software: Q-Chem, Functional: ωPBE[3], Basis set: 6-31G**
We sample over different values of ω with a step size of $0.01\, a_0^{-1}$ and calculate the HOMO eigenvalues ($\epsilon_{\mathrm{HOMO}}(\omega)$) and ionization potential (IP(ω)) for both the neutral system (N) and the anion (N+1). For each system, we fit a quadratic function into the difference between $\epsilon_{\mathrm{HOMO}}(\omega)$ and $-\mathrm{IP}(\omega)$. Those parabolas are used to evaluate $J^2(\omega)$ and we determine the value of ω that minimizes $J^2(\omega)$, yielding ω_{opt}. The minimum found by this procedure can vary by a few mili a_0^{-1} depending on the details of the fit, but such tiny differences in ω do not have a relevant impact on the physical observables.

1-TBP–1-NDI-silane

Geometry Optimization

Software: Q-Chem, Functional: M06-2X, Basis set: 6-31G**
Optimization thresholds: Gradient-Max $< 3 \cdot 10^{-4}$ a.u. & $\Delta E < 1 \cdot 10^{-6}$ a.u.

Binding energy

Software: Q-Chem, Functional: M06-2X, Basis set: 6-311++G**

Optimal tuning

Software: Q-Chem, Functional: ωPBE, Basis set: 6-31G**
We sample over different values of ω with a step size of $0.01\, a_0^{-1}$ and evaluate $J^2(\omega)$ according to the procedure described above and determine the optimal ω_{opt} that minimizes J^2.

Excited states

Software: Q-Chem, Functional: ωPBE, Basis set: 6-31G**

3-TBP–3-NDI-silane

Geometry Optimization

Software: Q-Chem, Functional: M06-2X, Basis set: 6-31G**
Optimization thresholds: Gradient-Max $< 3 \cdot 10^{-4}$ a.u. & $\Delta E < 1 \cdot 10^{-6}$ a.u.

Optimal tuning

Software: Q-Chem, Functional: ωPBE, Basis set: 6-31G**
We sample over different values of ω with a step size of $0.01\, a_0^{-1}$ and evaluate $J^2(\omega)$ according to the procedure described above and determine the value ω_{opt} that minimizes $J^2(\omega)$.

Excited states with difference densities

Software: TeraChem[4] (singlets), QChem (triplets), Functional: OT-ωPBE, Basis set: 6-31G*, Tamm-Dancoff approximation

2-TBP–2-NDI

Initial Geometry Optimization for the Optimal Tuning

Software: Q-Chem, Functional: M06-2X, Basis set: 6-31G**
Optimization thresholds: Gradient-Max $< 3 \cdot 10^{-4}$ a.u. & $\Delta E < 1 \cdot 10^{-6}$ a.u.

Optimal tuning

Software: Q-Chem, Functional: ωPBE, Basis set: 6-31G**
We sample over different values of ω with a step size of $0.01\, a_0^{-1}$ and evaluate the $J^2(\omega)$ value with ωPBE. The minimal value for $J^2(\omega)$ is achieved for $\omega = 0.15\, a_0^{-1}$.
The sampling rate is chosen comparatively coarse. The resulting physics, however, are expected to be reliable within this accuracy.

Refined Geometry Optimization for Excited States and Initial Born-Oppenheimer Dynamics Structure

Software: TeraChem, Functional: OT-ωPBE, Dispersion correction: D3[5], Basis set: 6-31G
Optimization thresholds: $\Delta E < 1 \cdot 10^{-6}$ a.u. & Gradient-RMS $< 3 \cdot 10^{-4}$ a.u. & Gradient-Max $< 4.5 \cdot 10^{-4}$ a.u. & Displace-RMS $< 1.2 \cdot 10^{-3}$ a.u. & Displace-Max $< 1.8 \cdot 10^{-3}$ a.u.

Excited states with difference densities

Software: TeraChem, Functional: OT-ωPBE, Dispersion correction: D3, Basis set: 6-31G*, Tamm-Dancoff approximation

Born-Oppenheimer Molecular Dynamics
Software: TeraChem, Functional: OT-ωPBE, Dispersion correction: D3, Basis set: 6-31G*, Tamm-Dancoff approximation

Charge separation and recombination
Software: QChem, Functional: OT-ωPBE (total energies, excited-state energies, and couplings) and M06-2X (geometry optimization), Basis set: 6-31G**, Tamm-Dancoff approximation (only for the S1 geometry optimization)

S2 Charge separation and recombination

For the calculations presented in the Section 2.3.3, the optimized geometries of the ground state (Q0) and first excited state (Q1) were obtained by DFT and TDDFT/TDA calculations, respectively, using the M06-2X functional and 6-31G(d,p) basis set. Both optimizations had as initial guess the DFT optimized geometry performed with the ωPBE+D3 functional and 6-31G(d,p) basis set presented in Section 2.3.1. The energies reported here and the FCD parameters listed in the main manuscript were obtained from full TDDFT calculations with the ωPBE functional and 6-31G(d,p) basis set using $\omega = 0.150$ bohr^{-1}.

Table S1: Energy shifts with respect to $E_{S0}^{Q0} = -122680.575$ eV of the ground state and first four excited states for optimized geometries at S0 and S1. The small differences between the excited states energies reported for Q0 here and in Tab. 3 of the main manuscript are due to minor distinctions between the optimized geometries obtained with the ωPBE+D3 and M06-2X functionals.

Geometry	ΔE(S0) (eV)	ΔE(S1) (eV)	ΔE(S2) (eV)	ΔE(S3) (eV)	ΔE(S4) (eV)
Q0	0.000	1.116	1.695	2.192	2.578
Q1	0.326	0.677	1.687	2.009	2.494

Fig. 1 presents the Huang-Rhys spectrum of the S1→S0 transition for 2-TBP–2-NDI system, dominated by high frequency vibrational modes ($\nu > 400$ cm^{-1}). The Huang-Rhys factors are calculated by:

$$S_k = \frac{\omega_k \Delta Q_k^2}{2\hbar} \tag{1}$$

where ΔQ_k is the mass-weighted projection between two electronic states along mode k, given by:

$$\Delta Q_k = \sum_{\mu=1}^{3N} L_{\mu k}\, \Delta R_\mu \tag{2}$$

where L_μ is the mass-weighted normalized frequency eigenvectors obtained at Q0 and ΔR_μ is the geometry displacement between Q0 and Q1. The vibrational frequencies and corresponding mass-weighted normalized frequency eigenvectors were obtained from harmonic vibrational DFT calculations performed in Q-Chem[1] using the M06-2X functional[2] and 6-31G(d,p) basis set.

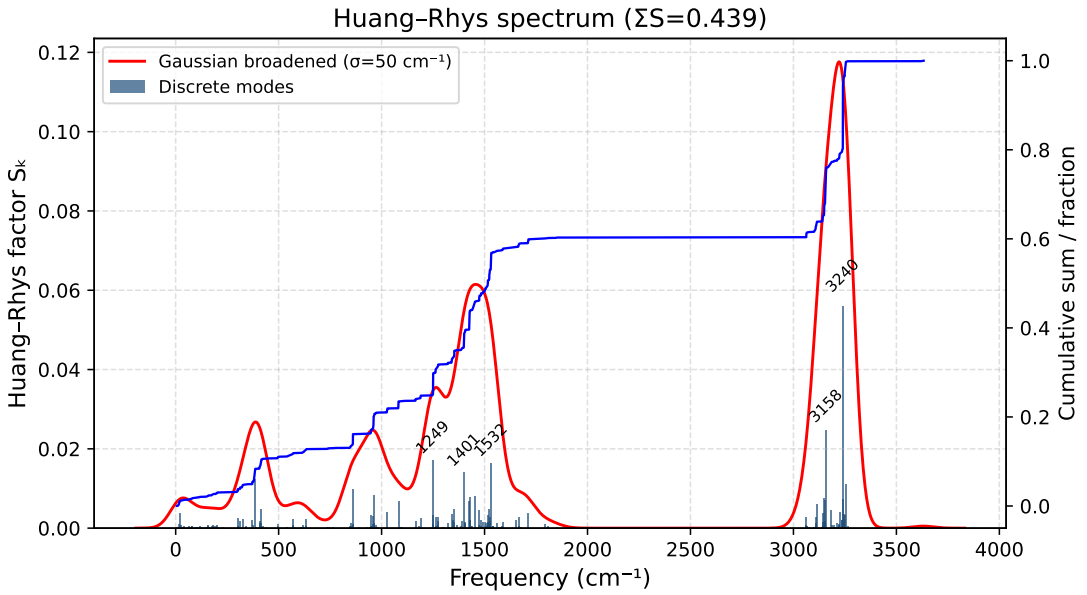

Figure S1: Huang-Rhys spectrum of the S1→S0 transition for the 2-TBP–2-NDI system.

S3 Experimental details

S3a NIR absorption spectroscopy

The vis-NIR absorption spectra were performed in a UV-M51 UV-vis-NIR single beam spectrometer (Bel Engineering) equipped with a tungsten and deuterium lamp and a silicon photodiode detector. The equipment can measure the absorption spectrum in the range of 190-1000 nm with 1 nm bandwidth. The measurements were performed in 2 mm thick quartz cuvettes.

S3b NMR spectroscopy

The NMR spectra were obtained in a Avance Neo 600 MHz Bruker spectrometer with magnetic flux of 14.1 T with a iProbe TBO 5mm BBF/19F/1H. The measurements were performed at 298 K with an acquisition time of 5 s collecting 12k points in the time dimension. The spectra were averaged over 32 scans. Further acquisition parameters are $\pi/2$ pulse of 12 μs (nutation frequency of 20.8 kHz). The ^{1}H single pulse experiments were performed applying a 30^o flip angle. The selective gradient-enhanced 1D ROESY experiments (selrogp Bruker protocol from - avance-version 21/09/15) were performed following an excitation $\pi/2$ pulse of 12 μs, a selective π gradient pulse of 12.2 ms and a spinlock ROESY pulse during (P15) 0, 200, and 900 ms. This methodology based on refs.

6–9 has been developed to contain no subtraction artifacts, such that NOE enhancements are detected with complete confidence.

Fig. 2 shows selected regions of the 1H NMR spectra of the TBP, NDI-silane and TBP/NDI-silane 2:1 THF-d8 solutions at a concentration of 30 g.L^{-1}. The frame c) shows the aromatic region (Ar), the frame a) the region around 8.56 ppm where the proton H4 of the NDI-silane is observed, and the frame b) shows the region around 6.8 ppm where the protons H3 and H5 of TBP are observed. The assigned peaks are labeled in correspondence to the structures presented in the inset of Fig. 2-c). For the NDI-silane in THF-d8 the assigned spectrum in δ (ppm) is: 0.59 (4H, H_α, m); 1.07 (18H, CH_3, t), 1.71 (4H, C_β, m), 3.69 (12H, OCH_2, q), 4.02 (4H, C_γ, t), and 8.57 (2H, Ar/H_4, s). For the TBP in THF-d8 the assigned spectrum in δ (ppm) is: 1.12 (18H, CH_3, s), 6.37 (2H, Ar/H2, d), 6.81 (2H, Ar/H_5, d), 6.83 (2H, Ar/H_3, dd), and 7.33 (1H, NH, s). Tetramethylsilane (TMS) is used as internal reference at 0.0000 ppm.

The singlet peaks due to THF are observed at 3.47 and 1.61 ppm with a maximum variation between the samples of 0.1 ppm (3 Hz). Interestingly, in the 2:1 TBP:NDI-silane mixture the peaks related to the Ar/H_4 of NDI-silane and Ar/H_5 of the TBP are about 12 Hz downshifted in comparison with the solutions of the separated molecules, which is beyond the variation in the chemical shift of the solvent. This is a result of an up-shielding effect on these sites, which is the first indication of their spatial interaction in the 2:1 TBP:NDI-silane THF solution.

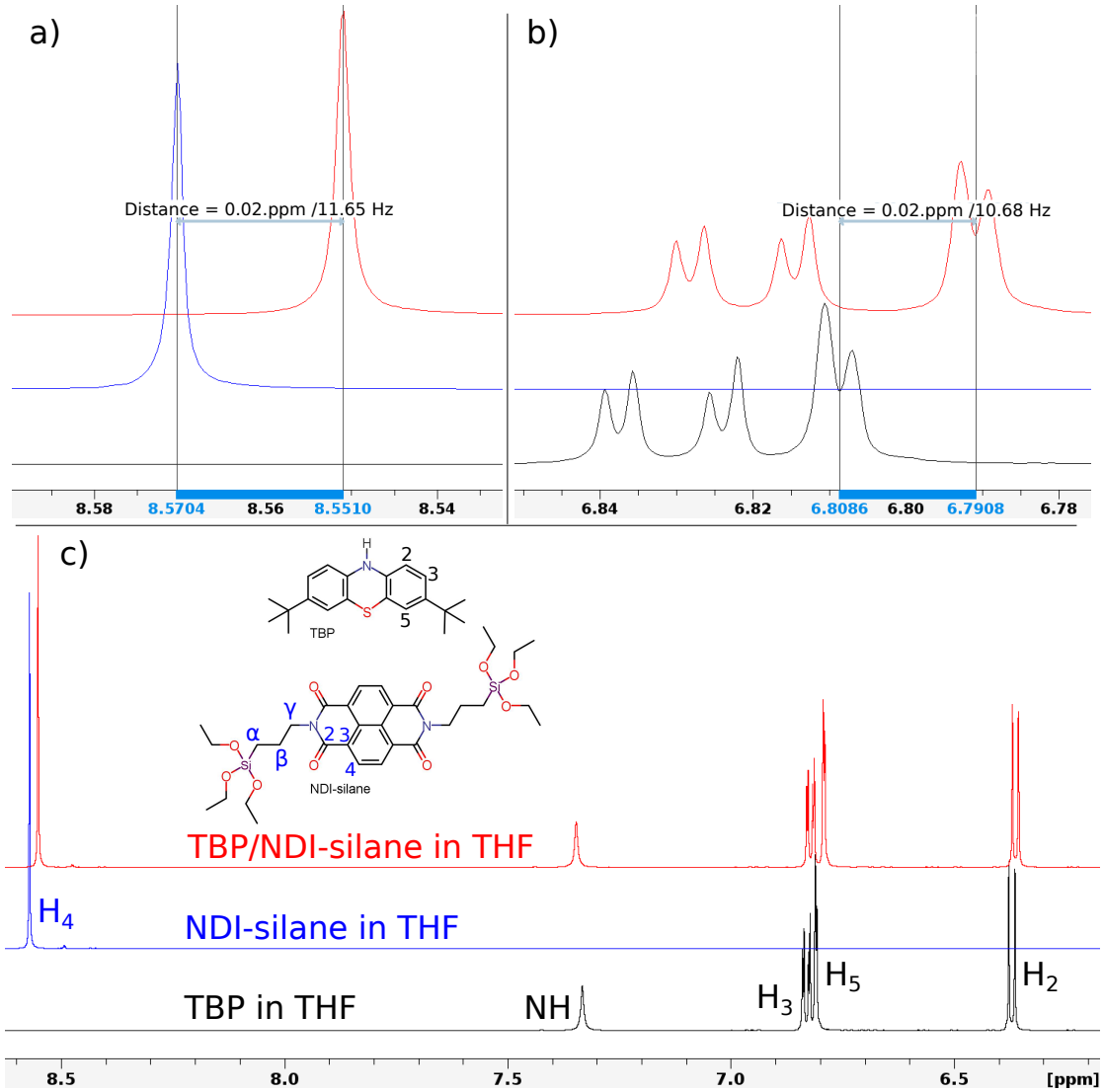

Figure S2: ^{1}H NMR spectra of the TBP, NDI-silane and TBP/NDI-silane 2:1 THF-d8 solutions, from bottom to top, at a concentration of 30 g.L^{-1}. Frame a) shows the region of the Ar/H_4 of the NDI-silane, frame b) the region of the Ar/H_3 and Ar/H_5 of the TBP, and frame c) shows the aromatic region.

Fig. 3 shows the ^{1}H selective 1D ROESY NMR spectra of the TBP/NDI-silane 2:1 THF-d8 concentrated solution with spin lock pulse duration of 0, 200, and 900 ms. The selective pulse is placed at 6.9 ppm, which excites only the protons Ar/H_3 and Ar/H_5 of the TBP molecule. The spectrum without spinlock pulse has no trace of signals due to NOE or spin-diffusion (as expected), neither zero-quantum coherence of a single pulse experiment, except for a tiny peak at 6.37 ppm corresponding to the (2H, Ar/H2, d) site of the TBP molecule. The spectrum obtained with spin lock pulse with duration of 200 ms has a significant negative-phase signal at 1.12 and 6.37 ppm, corresponding to the (18H, CH_3, s) and (2H, Ar/H2, d) protons of the TBP molecule, due to the NOE. Some traces of signal due to the NDI-silane could be observed already. The spectrum obtained with the spin lock pulse duration of 900 ms shows negative-phase peaks attributed to the TBP, due to NOE, and positive-phase peaks attributed to the NDI-silane. The positive-phase peaks are due to either chemical exchange or spin-diffusion (multiple spins cross correlation).10 In the case of the TBP with NDI-silane aggregates, it is reasonable to assume that chemical exchange is not relevant and that spin-diffusion is taking place.

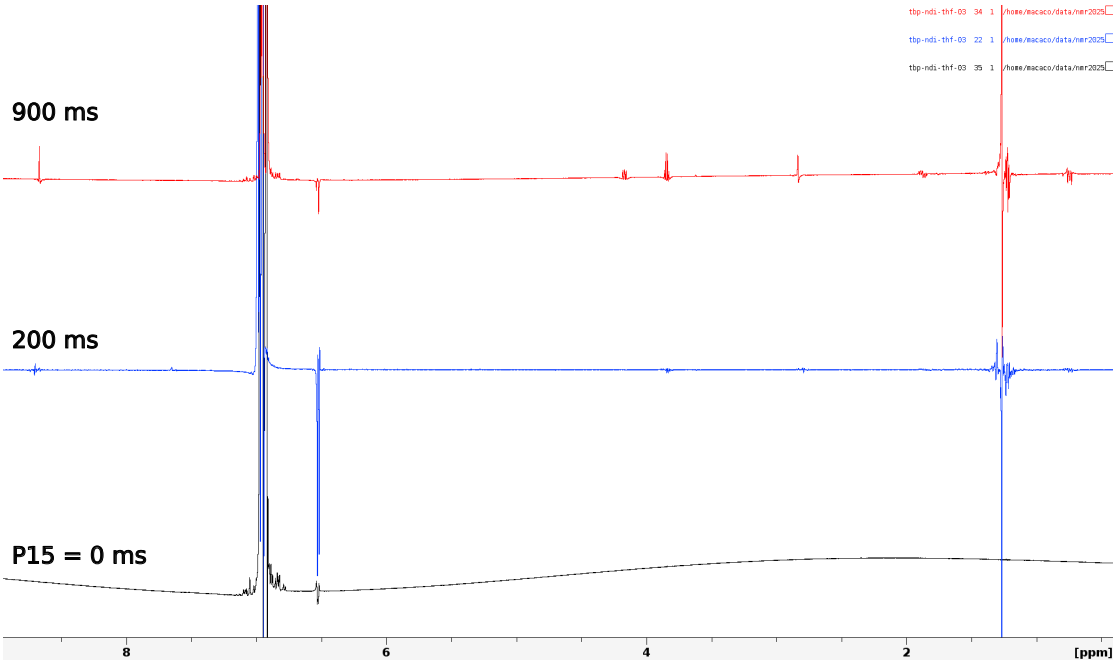

Figure S3: ^{1}H selective 1D ROESY NMR spectra of the TBP/NDI-silane 2:1 THF-d8 solution at a concentration of 30 g.L^{-1}. The spectra were taken with spin lock pulse duration of 0, 200, and 900 ms, from bottom to top, as indicated.

References

(1) E. Epifanovsky, A. T. B. Gilbert, X. Feng, J. Lee, Y. Mao, N. Mardirossian, P. Pokhilko, A. F. White, M. P. Coons, A. L. Dempwolff et al., Software for the

frontiers of quantum chemistry: An overview of developments in the Q-Chem 5 package, *J. Chem. Phys.*, 2021, **155**, 084801.

(2) Y. Zhao and D. G. Truhlar, The M06 Suite of Density Functionals for Main Group Thermochemistry, Thermochemical Kinetics, Noncovalent Interactions, Excited States, and Transition Elements: Two New Functionals and Systematic Testing of Four M06-class Functionals and 12 Other Functionals, *Theoretical Chemistry Accounts*, 2008, **120**, 215–241.

(3) O. A. Vydrov and G. E. Scuseria, Assessment of a Long-Range Corrected Hybrid Functional, *The Journal of Chemical Physics*, 2006, **125**, 234109.

(4) S. Seritan, C. Bannwarth, B. S. Fales, E. G. Hohenstein, C. M. Isborn, S. I. L. Kokkila-Schumacher, X. Li, F. Liu, N. Luehr, J. W. Snyder Jr. et al., TeraChem: A graphical processing unit-accelerated electronic structure package for large-scale ab initio molecular dynamics, *WIREs Computational Molecular Science*, 2021, **11**, e1494.

(5) S. Grimme, J. Antony, S. Ehrlich and H. Krieg, A Consistent and Accurate Ab Initio Parametrization of Density Functional Dispersion Correction (DFT-D) for the 94 Elements H-Pu, *The Journal of Chemical Physics*, 2010, **132**, 154104.

(6) H Kessler, H Oschkinat, C Griesinger and W Bermel, Transformation of homonuclear two-dimensional NMR techniques into one-dimensional techniques using Gaussian pulses, *Journal of Magnetic Resonance (1969)*, 1986, **70**, 106–133.

(7) J. Stonehouse, P. Adell, J. Keeler and A. J. Shaka, Ultrahigh-Quality NOE Spectra, *Journal of the American Chemical Society*, 1994, **116**, 6037–6038.

(8) K. Stott, J. Stonehouse, J. Keeler, T.-L. Hwang and A. J. Shaka, Excitation Sculpting in High-Resolution Nuclear Magnetic Resonance Spectroscopy: Application to Selective NOE Experiments, *Journal of the American Chemical Society*, 1995, **117**, 4199–4200.

(9) A. Bax and D. G. Davis, Practical aspects of two-dimensional transverse NOE spectroscopy, *Journal of Magnetic Resonance (1969)*, 1985, **63**, 207–213.

(10) A. Kumar, R. Christy Rani Grace and P. Madhu, Cross-correlations in NMR, *Progress in Nuclear Magnetic Resonance Spectroscopy*, 2000, **37**, 191–319.